

CLUSTER MULTIPOINT OBSERVATIONS OF IONIC STRUCTURES IN THE PLASMASPHERE BY CIS AND COMPARISON WITH IMAGE-EUV OBSERVATIONS AND WITH MODEL SIMULATIONS

I. Dandouras⁽¹⁾, V. Pierrard⁽²⁾, J. Goldstein⁽³⁾, C. Vallat⁽¹⁾,
G. K. Parks⁽⁴⁾, H. Rème⁽¹⁾, M. McCarthy⁽⁵⁾,
L. M. Kistler⁽⁶⁾, B. Klecker⁽⁷⁾, A. Korth⁽⁸⁾,
M.-B. Bavassano-Cattaneo⁽⁹⁾, P. Escoubet⁽¹⁰⁾, and A. Masson⁽¹⁰⁾

⁽¹⁾ Centre d'Etude Spatiale des Rayonnements, CNRS/UPS, Toulouse, France

⁽²⁾ Belgian Institute for Space Aeronomy, Brussels, Belgium

⁽³⁾ Southwest Research Institute, San Antonio, Texas, USA

⁽⁴⁾ Space Sciences Laboratory, UC Berkeley, California, USA

⁽⁵⁾ Geophysics, University of Washington, Seattle, Washington, USA

⁽⁶⁾ University of New Hampshire, Durham, NH, USA

⁽⁷⁾ Max-Planck-Institut für Extraterrestrische Physik, Garching, Germany

⁽⁸⁾ Max-Planck-Institut für Sonnensystemforschung, Katlenburg-Lindau, Germany

⁽⁹⁾ Istituto di Fisica dello Spazio Interplanetario, Rome, Italy

⁽¹⁰⁾ ESA/ESTEC RSSD, Noordwijk, The Netherlands

ABSTRACT

The 4 Cluster spacecraft orbit the Earth in a highly eccentric polar orbit at 4 R_E perigee, and this permits them to sample the ring current, the radiation belts and the outer plasmasphere. Data provided by the Cluster Ion Spectrometry (CIS) instruments are used to analyze Cluster crossings of the plasmasphere. CIS is capable of obtaining full three-dimensional ion distributions (about 0 to 40 keV/q) with a time resolution of one spacecraft spin (4 sec) and with mass-per-charge composition determination. In addition the CIS Retarding Potential Analyzer (RPA) allows more accurate measurements in the about 0 - 25 eV/q energy range, covering the plasmasphere energy domain. The low-energy ion distribution functions, obtained by CIS-RPA during the perigee passes, allow to reconstruct statistically the plasmopause morphology and dynamics, but they also reveal new and interesting features. The ion discrimination capability of CIS reveals how the density profile is different for each of the main ion species (H^+ , He^+ , O^+): H^+ and He^+ present mostly similar profiles; O^+ , however, is not observed as trapped plasmaspheric population at the Cluster orbit altitudes. Low-energy O^+ is observed mainly as upwelling ion, on auroral field lines. Detached plasmasphere events are also observed during some of the passes. The bi-directional distribution functions of these detached plasmaspheric populations allow us to distinguish them from upwelling ion populations. The CIS-RPA observations of the plasmopause position have been simulated with an interchange instability numerical model for the plasmopause deformations, and the model reproduces in a very satisfactory way the CIS observations. The CIS local ion measurements have also been correlated with global images of the plasmasphere, obtained by the

EUV instrument onboard Image, for an event where the Cluster spacecraft were within the field-of-view of EUV. The EUV images show that the difference observed between two Cluster spacecraft was temporal (boundary motion). They thus show the necessity for correlating local measurements with global images, and the complementarity of the two approaches; local measurements giving the “ground truth” (including plasma composition, distribution functions etc.) and global images allowing to put local measurements into a global context, and to deconvolve spatial from temporal effects.

1. INTRODUCTION

The plasmasphere is the torus of cold and dense plasma, which encircles the Earth at geomagnetic latitudes less than about 65° , occupying the inner magnetosphere out to a boundary known as the plasmopause. There, the density can drop by 1 to 2 orders of magnitude. The configuration and dynamics of the plasmasphere are highly sensitive to geomagnetic disturbances. During extended periods of relatively quiet geomagnetic conditions the outer plasmasphere can become diffuse, with a gradual fall-off of plasma density. During increasing magnetospheric activity, however, the plasmasphere is eroded and plasmaspheric ions can be peeled off and escape toward the outer magnetosphere. The outer plasmasphere region is located at the interface between the expanded ionosphere, corotating with the Earth, and the internal magnetosphere, dominated by sunward convection [e.g. 1]. In contrast with the inner plasmasphere, where the density repartition is smooth, the outer plasmasphere is characterised by complex

plasma structures, formed by fluctuations of the convective large-scale electric field governed by solar wind conditions.

Data provided by the Cluster Ion Spectrometry (CIS) experiment [2] are used here to analyse the ionic structures observed locally during the Cluster spacecraft crossings of the plasmasphere. The perigee of the four Cluster spacecraft, at $\sim 4 R_E$, allows cuts through the outer plasmasphere. The CIS observations of the plasmopause position are then compared to the simulation results using an interchange instability numerical model for the plasmopause deformations [3]. The CIS local ion measurements have also been correlated with global images of the plasmasphere, obtained by the EUV instrument onboard Image [4], for an event where the Cluster spacecraft were within the field-of-view of EUV.

An extended description of the ionic structures observed in the outer plasmasphere by the CIS experiment, and how they compare with observations by EUV and with model simulations, is given in reference [5]. Here we present a summary of the main features observed.

2. THE CIS EXPERIMENT

The CIS (Cluster Ion Spectrometry) experiment is a comprehensive ionic plasma spectrometry package onboard the four Cluster spacecraft, capable of obtaining full three-dimensional ion distributions with a time resolution of one spacecraft spin (4 sec) and with mass-per-charge composition determination [2].

The CIS package consists of two different instruments, a time-of-flight ion Composition and Distribution Function analyser (CODIF, or CIS-1) and a Hot Ion Analyser (HIA, or CIS-2). The mass-resolving spectrometer CODIF provides the ionic composition of the plasma for the major magnetospheric species, from the thermal energy to about 40 keV/q. In addition CODIF is equipped with a Retarding Potential Analyser (RPA), which allows more accurate measurements in the about 0.7 - 25 eV/q energy range (with respect to the spacecraft potential), covering the plasmasphere energy domain. The operation on CODIF of the RPA mode and of the normal magnetospheric modes (which provide a 25 eV/q to 40 keV/q energy range) is mutually exclusive. The RPA mode is thus operated on one out of 10 orbits, on the average, and not always on all of the spacecraft.

3. OBSERVATIONS

3.1 Plasmasphere Cut Example

Figure 1 shows an example of a Cluster crossing of the plasmasphere, in the post-noon sector (15:30 MLT),

during quiet magnetospheric conditions ($K_p = 1+$). During this event CODIF (bottom 3 spectrograms in Figure 1) was in the RPA mode ($\sim 0.7 - 25$ eV/q) until 16:00 UT, when it switched back to a normal magnetospheric mode (full energy coverage). HIA (top spectrogram in Figure 1) was continuously in a normal magnetospheric mode. Cluster was in the southern lobe until $\sim 10:20$ UT, when it crossed a first boundary, entering into the southern plasma sheet (cf. HIA data). At $\sim 10:45$ UT the spacecraft entered into the ring current, where it remained until $\sim 13:40$ UT, characterized in these data by intense particle fluxes at energies above 7 keV, showing the presence of high-energy ions subject to gradient and curvature drift [6]. The spacecraft then traversed through the northern plasma sheet and entered into the northern lobe, at the outbound leg of its trajectory, at $\sim 14:38$ UT.

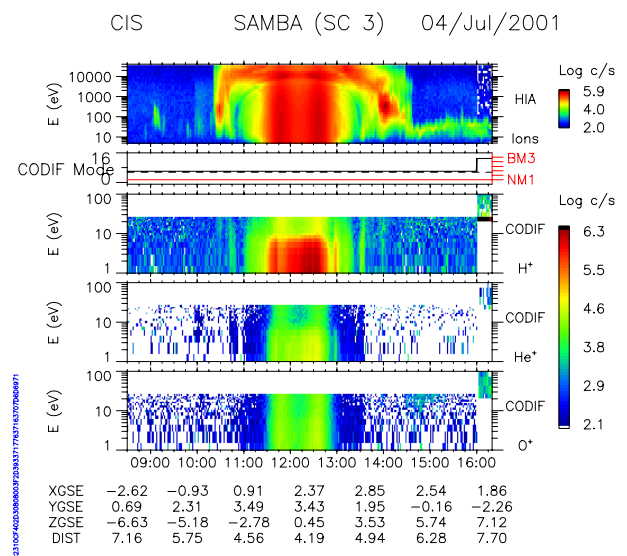


Fig. 1. Cluster spacecraft 3 ion data for July 4, 2001. From top to bottom: HIA energy-time ion spectrogram (normal magnetospheric mode: 5 eV/q – 32 keV/q), in corrected-for-detection-efficiency counts per sec. (c/s); CODIF mode (in black: RPA mode until 16:00 UT); CODIF Energy-time ion spectrograms, separately for H^+ , He^+ , and O^+ ; spacecraft coordinates (GSE system) and geocentric distance, in R_E . From reference [5].

Between 11:30 and 12:55 UT HIA suffered a strong background due to penetrating particles from the radiation belts, appearing as a high counting rate at all energies. This background presents two maxima centered on L-shell values around 4.5, one at the inbound leg and the other at the outbound leg of the orbit. CODIF, which during this orbit interval was in the RPA mode, first detected the presence of a diffuse low-energy ion population at 11:00 UT, and then entered the main plasmasphere at 11:30 UT. This is characterized by high ion fluxes at energies below 7.7 eV/q, with respect to the spacecraft potential (which in the plasmasphere is of the order of 1-2 V). The plasmaspheric ion data shown here cover thus an energy

domain of ~ 2 to ~ 9 eV, and they correspond to the tail of the distribution function, which in the plasmasphere has typical temperatures of the order of 1 eV.

3.2 Detached Plasmasphere Observations

Figure 2 shows a crossing of the plasmasphere by Cluster spacecraft (sc) 1, 3 and 4, in the morning sector (08:45 MLT), during initially quiet magnetospheric conditions (31 October 2001 event: $K_p = 0+$ during the 9-12 UT interval). The onset of a negative auroral bay is however observed in the AE index at $\sim 12:30$ UT, i.e. close to the outbound plasmopause crossing by the Cluster spacecraft, and the K_p index jumped from $0+$ to 3 in the 12-15 UT interval.

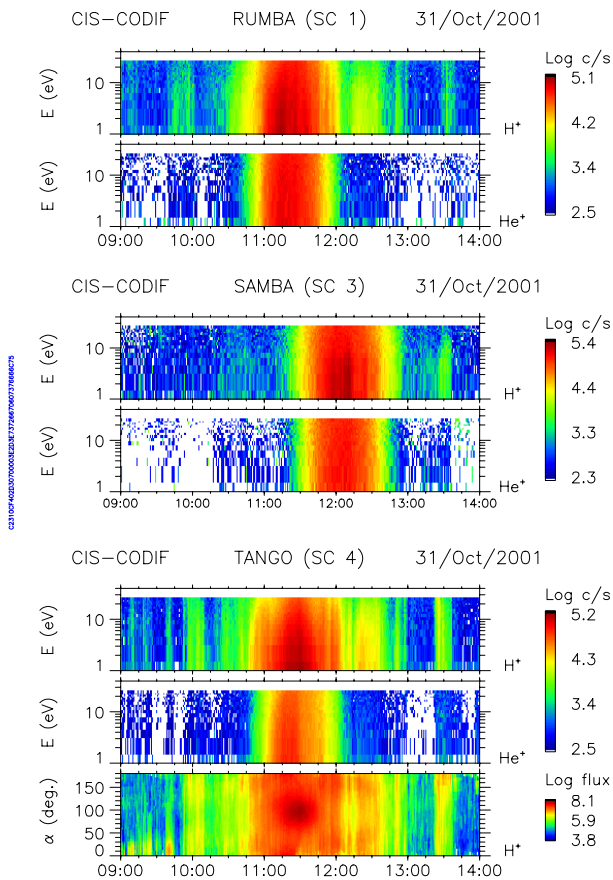


Fig. 2. Cluster H^+ and He^+ energy-time ion spectrograms, in corrected-for-detection-efficiency counts per sec., for October 31, 2001. All spacecraft in RPA mode. Bottom panel: sc 4 pitch-angle distributions for H^+ ions (~ 0.7 eV/q to 25 eV/q energy range), in particle flux units ($\text{cm}^{-2} \text{sr}^{-1} \text{s}^{-1} \text{keV}^{-1}$).

From reference [5].

All spacecraft were in the RPA mode. Cluster sc 3 was lagging on its orbit, with respect to the other spacecraft, which explains why it crossed the plasmasphere about 30 minutes later. Sc 1 and 4 crossed the plasmaspheric main ion population between $\sim 10:47$ UT ($L \approx 5.1$) and

$\sim 12:04$ UT ($L \approx 5.8$). However, detached plasma of lower density was also observed before the entry into the main plasmasphere, at around 10:00 UT ($L \approx 11$), and after the exit from the plasmasphere, at around 12:25 UT ($L \approx 8$) and at around 13:30 UT.

The bottom panel of Figure 2 shows the H^+ pitch-angle distributions (pad) for sc 4. The distributions in the main plasmasphere are relatively isotropic, while around the crossing of the equatorial plane the major part of the proton population is centred at 90° (pancake distributions). On the detached plasmasphere observations, however, the distributions are still trapped (distributions symmetric with respect to the magnetic field), but are of the butterfly type, presenting a deficiency of particles perpendicular to the magnetic field direction.

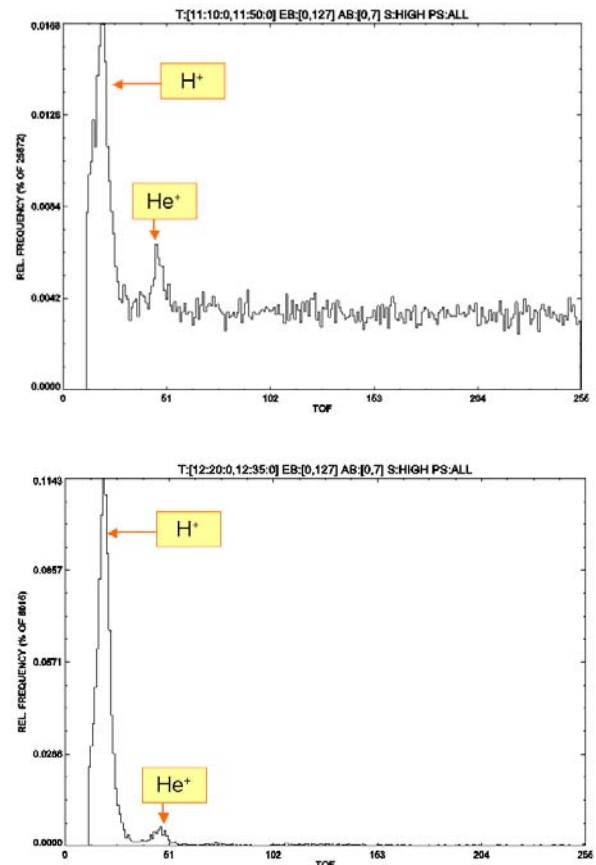


Fig. 3. Time-of-flight spectra, for the ions detected during the October 31, 2001 event, for two intervals (see text). The abscissa is the time-of-flight channel number (inversely proportional to the ion velocity).

Figure 3 shows the time-of-flight spectra for two intervals, corresponding to (from top to bottom): 11:10 - 11:50 UT (main plasmasphere) and 12:20 - 12:35 UT (detached plasmasphere). A persistent background due to penetrating particles from the radiation belts is present in the first spectrum, obtained in the main

plasmasphere. For the following spectrum, however, corresponding to the detached plasmasphere observations in the outbound leg of the orbit, the background disappears. These spectra show the absence of O^+ ions. All spectra show the characteristic peaks of H^+ and He^+ .

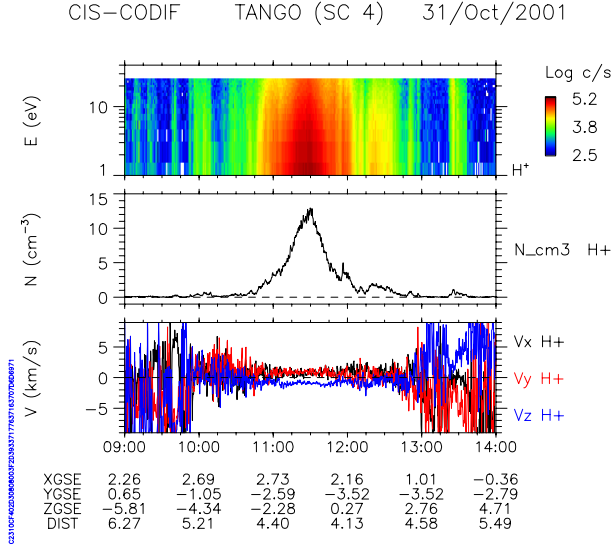


Fig. 4. Cluster sc 4 CODIF H^+ data for October 31, 2001. From top to bottom: Energy-time ion spectrogram and moments of the distribution functions (~ 0.7 eV/q to 25 eV/q energy range): density, velocity (in GSE coordinates).

The moments of the ion distribution functions of H^+ , calculated in the ~ 0.7 eV/q to 25 eV/q energy range (with respect to spacecraft potential), are shown in Figure 4. The density values measured during the detached plasmasphere observations are by about an order of magnitude lower than the ones measured in the main plasmasphere, consistently with the substantial density reduction for the detached plasma shells predicted by the peeling-off models [7]. The H^+ velocities measured here show a clear $V_x > 0$ and a $V_y > 0$ component in the main plasmasphere ($\sim 11 - 12$ UT), corresponding to a corotating plasma (08:45 MLT). For the detached plasmasphere observations, however, around 13:30 UT, the measured velocities are dominated by $V_y < 0$ and $V_z > 0$, showing a strong outward expansion of the plasma tube. This expansion velocity increases as a function of the L-shell value.

3.3 Cluster Multi-Spacecraft Plasmasphere Observations and Modeling

In the first six months of 2002 the Cluster inter-spacecraft separation was reduced so as to obtain a regular tetrahedron of a 100 km characteristic size when traversing the cusp. This resulted in an elongated tetrahedron, of ~ 70 km width and ~ 240 km height mainly along the GSE z-axis, when crossing perigee.

Figure 5 shows a crossing of the plasmasphere by Cluster sc 1, 3 and 4, in the night sector (00:45 MLT), during moderately disturbed magnetospheric conditions ($K_p = 2$, $AE \approx 200$ nT). Sc 1 and 3 were in the main plasmasphere between $\sim 21:32$ UT ($L \approx 4.3$) and $\sim 22:02$ UT ($L \approx 4.2$). Sc 4, however, did not at all detect the main plasmasphere, but only a low-density cold plasma, revealing the close presence of the plasmopause and the associated density gradient. The separation between sc 3 and sc 4, projected in the equatorial plane, was only 65 km. This gives a measure of the density gradients in the vicinity of the plasmopause, the density measured by sc 4 being lower by a factor of the order of 50-100 with respect to the one measured by sc 3. Note that the H^+ gyroradius at this region, for 2 eV plasmaspheric ions, is 0.6 km, i.e. consistent with the density gradients observed.

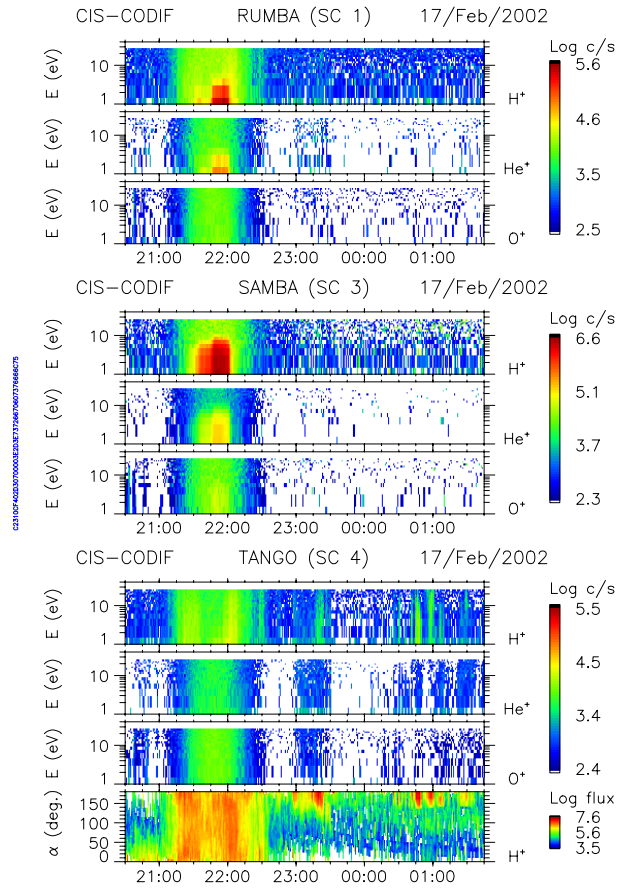


Fig. 5. Cluster sc 1, 3 and 4 H^+ , He^+ and O^+ energy-time ion spectrograms. All spacecraft in RPA mode. Bottom panel: sc 4 pitch-angle distributions for H^+ ions (~ 0.7 eV/q to 25 eV/q energy range), in particle flux units ($\text{cm}^{-2} \text{sr}^{-1} \text{s}^{-1} \text{keV}^{-1}$). From reference [5].

This localisation of the plasmopause, between the closely spaced Cluster spacecraft, allows us to compare the observation with model predictions. The interchange instability numerical model for the plasmopause deformations [3] was used here to simulate the February

17, 2002 event. This model uses as input an empirical Kp-dependent equatorial electric field model [8], and it determines, using kinetic simulations, the plasmapause position as the location where plasma interchange peels off the plasmasphere, i.e., where and when the magnetospheric convection velocity is enhanced at the onset of substorms [7]. According to this physical mechanism, the plasmapause is formed in the post-midnight MLT sector where and when the field-aligned component of the centrifugal pseudo-force overcomes that of the gravitational force.

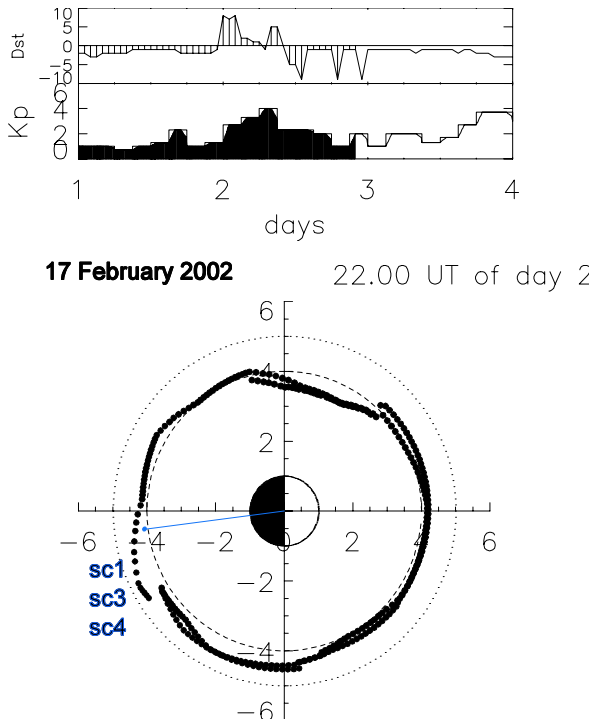


Fig. 6. Numerical simulation results of the plasmapause deformations, for the 17 February 2002 event, using the interchange instability model. Upper panel: Kp index time history, used as input parameter for the simulation.

Bottom panel: simulation results of the plasmapause deformations, in the equatorial plane. The blue dot corresponds to the Cluster spacecraft positions (sc 1, 3 and 4), which appear as a single dot due to their close spacing. From reference [5].

The simulation results appear in Figure 6, bottom panel (equatorial plane). The blue dot corresponds to the Cluster spacecraft position (sc 1, 3 and 4), which appear as a single dot due to their close spacing: less than 100 km. It appears clearly that the spacecraft are almost at the edge of a plasmapause bulge, formed by plasma brought by the interchange instability. This explains why only some of the spacecraft (1 and 3) entered the plasmasphere.

The February 17, 2002 plasmasphere observation included also an eclipse which, for example for sc 3, was between 21:46 UT and 22:09 UT (cf. Figure 7). The

suppression of photoelectron production allows us to evaluate the change in the spacecraft potential. The entrance in the plasmasphere (for sc1 and 3) is well before the start of the eclipse, and the exit from the plasmasphere (for sc1 and 3) is during the eclipse. The depth of the eclipse is almost the same for all sc. The only effect of the eclipse on the low-energy ions, detected by CIS-RPA, is a slight enhancement of the detected ion fluxes, and an increase in their energy by 1-2 eV, due to a more negative spacecraft potential by 1-2 V. This is consistent with the spacecraft potential measurements by the EFW electric field experiment onboard Cluster [9]. In the low-density magnetospheric lobes, however, the spacecraft potential can become positive by several Volts or even tens of Volts, unless the ASPOC ion emitter [10], used for the spacecraft active potential control, is operating.

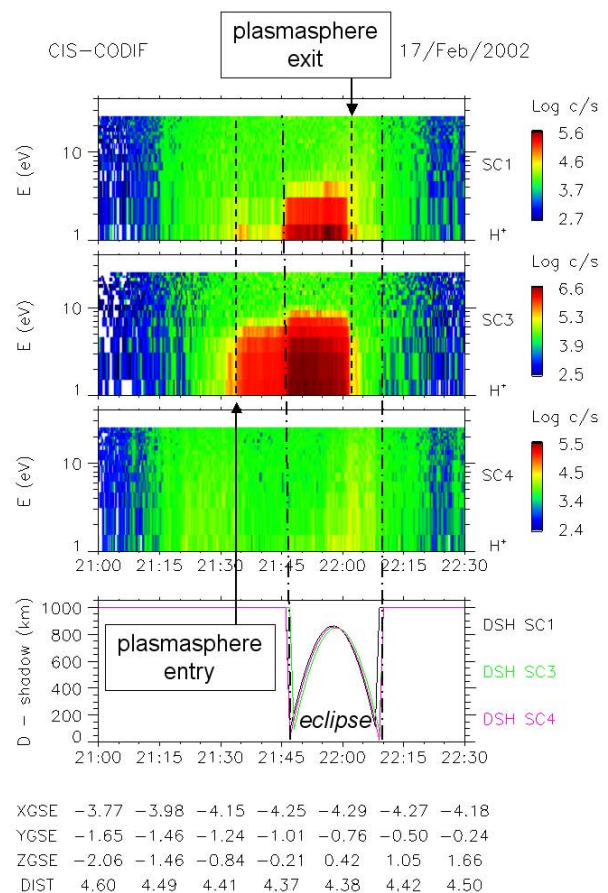


Fig. 7. Cluster sc 1, 3 and 4 H⁺ energy-time ion spectrograms, for February 17, 2002. The bottom panel shows an indicator of the spacecraft penetration within the eclipse shadow cone.

At the outbound leg, around 01:00 UT (February 18, 2002) sc 4 detected three successive spikes of low-energy H⁺ ions. As the pitch-angle distributions of these ions show (bottom panel of Figure 5), these are upwelling ions escaping from the ionosphere along the magnetic field lines. Their composition included only

H^+ and He^+ , and no O^+ , as can be deduced from the time-of-flight spectrum (not shown). It should be noted that the ASPOC ion emitter was operating, on sc 4, during this interval.

3.4 Cluster and Image Correlated Plasmasphere Observations

On August 9, 2001, the Cluster spacecraft went through perigee in the noon sector (13:30 MLT), during the onset of a negative magnetic bay in the auroral zone (max AE = 500 nT, $K_p = 2$), following a long period of quiet conditions ($K_p = 1$ for several hours). Sc 3 was in the plasmasphere between ~04:50 UT ($L \approx 4.4$) and ~05:50 UT ($L \approx 5.3$). Sc 1, however, did not at all detect the main plasmasphere, and the only signature in the particle data is increased background from the radiation belts, also seen by sc 3 (Figure 8). It should be noted that, as shown in Figure 9, sc 1 was leading on the orbit by 45 minutes: sc 1 went through perigee at 04:18 UT and sc 3 at 05:03 UT. The sc 3 orbit got also deeper into the inner magnetosphere, with a minimum L-shell value of 4.2, versus 4.3 minimum L for sc 1.

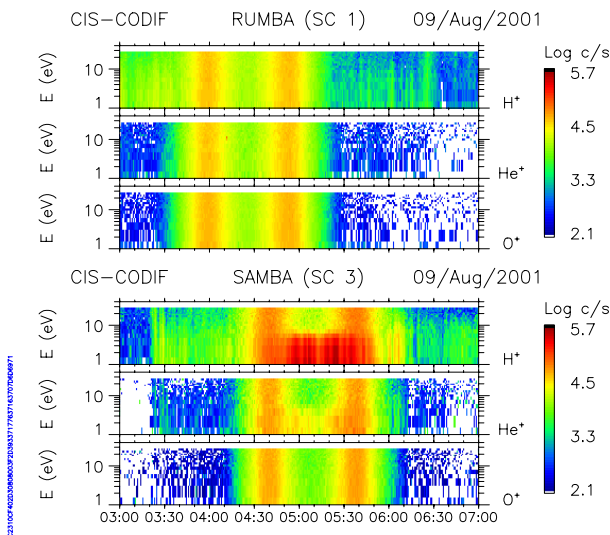


Fig. 8. Cluster sc 1 and 3 H^+ , He^+ and O^+ energy-time ion spectrograms, for August 9, 2001. Both spacecraft in RPA mode.

In order to interpret the difference in observations between these two Cluster spacecraft (the only ones operating in the RPA mode during this event), and to deduce whether it was due to spatial effects (plasmopause situated between the trajectories of sc 1 and sc 3), or to temporal effects (boundary motion), we examined the plasmaspheric images provided by the EUV experiment onboard the Image spacecraft [4].

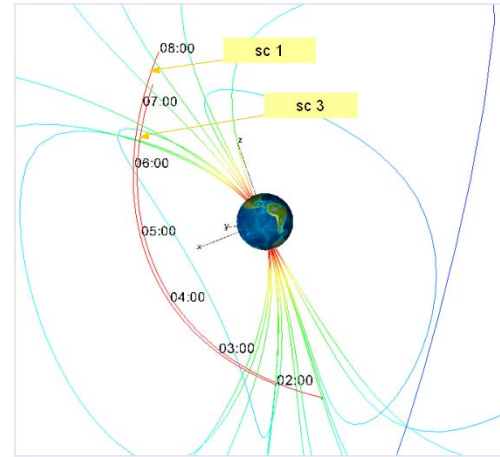


Fig. 9. Cluster sc 1 and 3 orbits for August 9, 2001, projected on the Tsyganenko 89 magnetic field model. Orbit Visualization Tool plot, courtesy of the OVT Team.

Figure 10 shows such an image, acquired at 04:21 UT. What appears in these images is a very diffuse plasmasphere, with a gradual fall-off of the plasma density and no clear plasmopause boundary, and also a lot of azimuthal variation. This resulted from the extended period of relatively quiet geomagnetic conditions, preceding the observations. It is possible, however, to define an ad-hoc plasmopause as where there is a gradient in intensity that passes through 100 or so [11].

The above definition of an ad-hoc plasmopause has been used to produce the white dotted line plots in the two panels of Figure 11, which show the intensity of the EUV 30.4 nm emissions at 13.5 MLT, as a function of UT and L . The projected sc 1 or sc 3 orbit is indicated with the blue or green curve, respectively, in the two panels.

These panels show a temporal dependence of the radial extent of the plasmasphere at 13.5 MLT. Sc 1 goes through 13.5 MLT when the ad-hoc plasmopause is just at about $L = 4.2$, just skimming above it. Sc 3 passes through 13.5 MLT when the ad-hoc plasmopause (at this MLT) has moved outward to $L \approx 4.8$, passing well inside of it. This is consistent with the in-situ observation of the plasmasphere by sc 3, and the absence of plasmasphere detection by sc 1 (cf. Figure 8).

The outward motion of the plasmopause at 13.5 MLT, between the perigees of sc 1 and sc 3, is not a result of dynamic expansion of the global plasmopause. It results rather from the fact that the radial density profile of the plasmasphere varies with MLT, and a more extended radial profile “rotated” into 13.5 MLT in between the sc 1 and sc 3 perigees, due to the plasmasphere co-rotation with the Earth. Because there is so much

azimuthal structure in the plasma density, this caused a slightly larger radial extent of the dense plasma to rotate into 13.5 MLT.

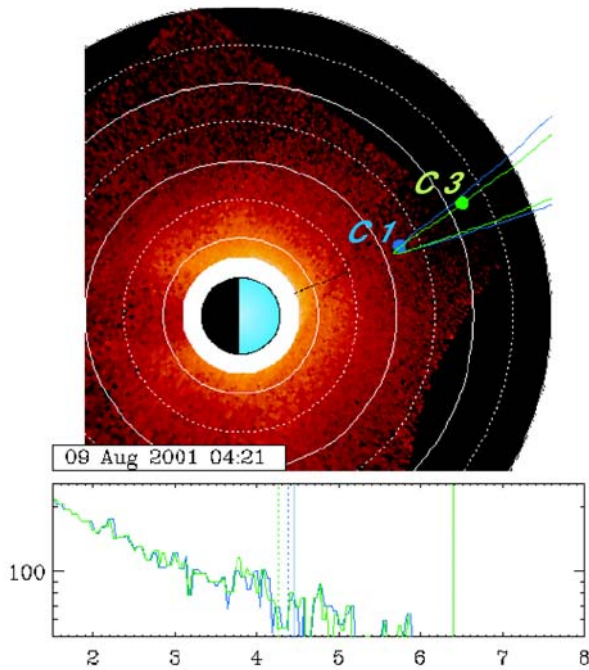


Fig. 10. EUV images of the plasmasphere, for August 9, 2001. The top panel shows the projection in the magnetic equatorial plane. The reddish haze around the Earth is EUV-observed 30.4 nm emissions from He^+ .

The blue and green lines are the Cluster sc 1 and 3 orbits (respectively), mapped to the equator. The dot shows where each satellite is at 04:21 UT. The bottom panel shows radial slices through the EUV equatorial image, with the vertical axis being intensity (from 0-255) and the horizontal axis being L-shell. The blue curve is a radial intensity slice at the Cluster sc 1 perigee MLT and the green curve is for sc 3. The vertical dotted lines mark the perigee L-shell of each spacecraft. The vertical solid lines show the instantaneous L-positions of each spacecraft.

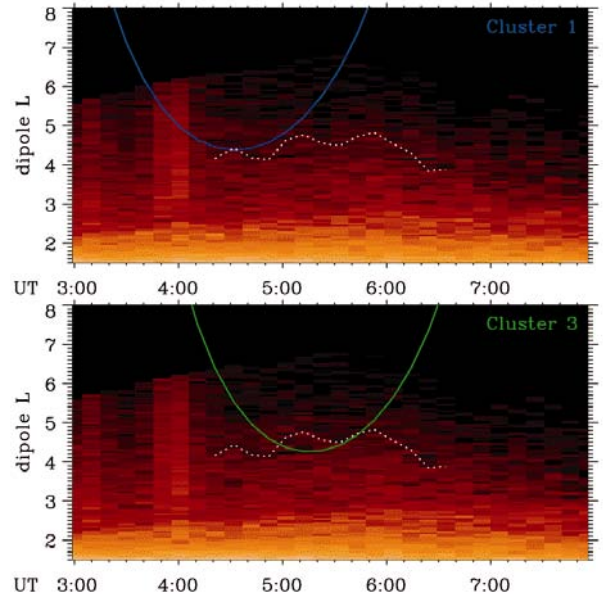


Fig. 11. Two panels of Image-EUV data (upper and lower, one for each Cluster spacecraft sc1 and sc3). In each panel the colour corresponds to the intensity of the EUV 30.4 nm emissions at 13.5 MLT, as a function of UT and L . The projected sc 1 or sc 3 orbit is indicated with the blue or green curve, respectively. The ad-hoc plasmapause L -value (see text) is the white dotted line. The intervals [2:59, 3:10, 3:51, 4:01, 4:11] correspond to high background noise. From reference [5].

4. DISCUSSION AND CONCLUSIONS

We have analysed some typical events, representative of the ionic structures observed in or close to the outer plasmasphere by the CIS experiment onboard the Cluster spacecraft [2]. From our analysis, we can conclude that:

- The H^+ and He^+ ions show mostly similar density profiles, with the He^+ densities being much lower. O^+ ions, however, are not observed as part of the main plasmaspheric population at the Cluster orbit altitudes ($R \geq 4 R_E$). Low-energy ($E < 25$ eV) O^+ is observed only as upwelling ions, escaping from the ionosphere along auroral field lines.
- Detached plasmasphere events, that are observed by CIS during some of the passes at about 0.5 to 1 R_E outside of the plasmapause, are also present. The symmetric bi-directional pitch-angle distribution functions of these detached plasmaspheric populations allow us to distinguish them from upwelling ion populations.
- The density values measured in the detached plasmasphere observations are by about an order of magnitude lower than the ones measured in the main plasmasphere, consistently with the substantial density reduction for the detached

plasma shells predicted by the peeling-off models [7].

- The plasmasphere co-rotation with the Earth is observed in the ion distribution functions, acquired within the main plasmasphere. In the detached plasmasphere observations, however, the plasma is not corotating, but has a strong outward expansion velocity, which is increasing as a function of the L-shell value.
- The pitch-angle distributions in the main plasmasphere are relatively isotropic, while around the crossing of the equatorial plane the major part of the proton population is centred at 90° (pancake distributions). At higher latitudes and in the detached plasmasphere observations, however, the distributions are of the butterfly type, presenting a deficiency of particles perpendicular to the magnetic field direction.
- The CIS-RPA observations of the plasmopause position have been simulated with an interchange instability numerical model for the plasmopause deformations [3], that uses as input an empirical Kp-dependent equatorial electric field model [8]. The numerical model reproduces in a very satisfactory way the CIS observations.
- The CIS local ion measurements have been also correlated with global images of the plasmasphere, obtained by the EUV instrument onboard Image [4], for an event where the Cluster spacecraft were within the field-of-view of EUV. The EUV images show, for this event, that the difference observed between two Cluster spacecraft was temporal (boundary motion): the radial density profile of the plasmasphere varies with MLT, and a more extended radial profile “rotated” in between the two Cluster spacecraft perigee passes. They thus show the necessity for correlating local measurements with global images, and the complementarity of the two approaches; local measurements giving the “ground truth” (including plasma composition, distribution functions etc.) and global images allowing to put local measurements into a global context, and to deconvolve spatial from temporal effects.

REFERENCES

1. Lemaire J.F. and Gringauz K.I., with contributions from Carpenter D.L. and Bassolo V., *The Earth's Plasmasphere*, Cambridge University Press, Cambridge, 1998.
2. Rème H., et al., First multispacecraft ion measurements in and near the Earth's magnetosphere with the identical Cluster ion spectrometry (CIS) experiment, *Ann. Geophys.*, Vol. 19, 1303, 2001.
3. Pierrard V. and Lemaire J.F., Development of shoulders and plumes in the frame of the interchange instability mechanism for plasmopause formation, *Geophys. Res. Lett.*, 31, L05809, doi: 10.1029/2003GL018919, 2004.
4. Sandel B.R., et al., The extreme ultraviolet imager investigation for the IMAGE mission, *Space Science Reviews*, 91, 197–242, 2000.
5. Dandouras I., Pierrard V., Goldstein J., Vallat C., Parks G. K., Rème H., Gouillart C., Sevestre F., McCarthy M., Kistler L. M., Klecker B., Korth A., Bavassano-Cattaneo M. B., Escoubet P., and Masson A., Multipoint observations of ionic structures in the Plasmasphere by CLUSTER-CIS and comparisons with IMAGE-EUV observations and with Model Simulations, *AGU Monograph: Inner Magnetosphere Interactions: New Perspectives from Imaging*, 159, 23-54, 2005.
6. Vallat C., Dandouras I., C:son Brandt P., Mitchell D.G., Roelof E.C., deMajistre R., Rème H., Sauvaud J.-A., Kistler L., Mouikis C., Dunlop M., and Balogh A., First comparisons of local ion measurements in the inner magnetosphere with ENA magnetospheric image inversions: Cluster-CIS and IMAGE-HENA observations, *J. Geophys. Res.*, 109, A04213, doi: 10.1029/2003JA010224, 2004.
7. Lemaire J. F., The formation of the light-ion trough and peeling off the plasmasphere, *J. Atmosph. Sol.-Terr. Phys.*, 63, 1285-1291, 2001.
8. McIlwain C.E., A Kp dependent equatorial electric field model, The Physics of Thermal plasma in the magnetosphere, *Adv. Space Res.*, 6(3), 187–197, 1986.
9. Gustafsson G.M., et al., First results of electric field and density observations by Cluster EFW based on initial months of operation, *Ann. Geophys.*, 19, 1219 - 1240, 2001.
10. Torkar K., et al., Active spacecraft potential control for Cluster – implementation and first results, *Ann. Geophys.*, 19, 1289 - 1302, 2001.
11. Goldstein J., Spasojević M., Reiff P.H., Sandel B.R., Forrester W.T., Gallagher D.L., and Reinisch B.W., Identifying the plasmopause in IMAGE EUV data using IMAGE RPI in situ steep density gradients, *J. Geophys. Res.*, 108, 1147, doi: 10.1029/2002JA009475, 2003.

COPYRIGHT:

This paper is based on [5], which is copyright 2005 American Geophysical Union.

Modified by permission of American Geophysical Union.